

Linear Correlation between Water Adsorption Energies and Volta Potential Differences for Metal/water Interfaces

Xiang-Ying Li, Ao Chen, Xiao-Hui Yang, Jia-Xin Zhu, Jia-Bo Le,* and Jun Cheng*



Cite This: *J. Phys. Chem. Lett.* 2021, 12, 7299–7304



Read Online

ACCESS |



Metrics & More

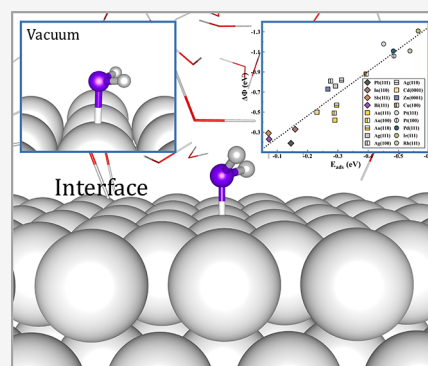


Article Recommendations



Supporting Information

ABSTRACT: Potential of zero charge (PZC) is an important reference for understanding the interface charge and structure at a given potential, and its difference from the work function of metal surface (Φ_M) is defined as the Volta potential difference ($\Delta\Phi$). In this work, we model 11 metal/water interfaces with ab initio molecular dynamics. Interestingly, we find $\Delta\Phi$ is linearly correlated with the adsorption energy of water (E_{ads}) on the metal surface. It is revealed that the size of E_{ads} directly determines the coverage of chemisorbed water on the metal surface and accordingly affects the interface potential change caused by electron redistribution ($\Delta\Phi_{\text{el}}$). Moreover, $\Delta\Phi$ is dominated by the electronic component $\Delta\Phi_{\text{el}}$ with little orientational dipole contributing, which explains the linear correlation between $\Delta\Phi$ and E_{ads} . Finally, it is expected that this correlation can be helpful for effectively estimating the $\Delta\Phi_{\text{el}}$ and PZC of other metal surfaces in the future work.



Metal/water interfaces are typical places for energy conversion between electricity and chemicals, in which, electrocatalytic reactions, such as hydrogen evolution reaction (HER),^{1–4} oxygen reduction reaction (ORR),^{5–8} and CO₂ reduction reaction (CO₂RR)^{9–12} occur. A fundamental property of metal/water interfaces is the potential of zero charge (PZC).^{13–16} This term was coined by Frumkin,¹⁵ and it is defined as the potential at which the electrode surface bears no net charge. Note that when the applied potential deviates from PZC, the interfaces will start to build up electric double layers. Therefore, PZC is the potential reference that can be used to determine the sign and amount of the charge on the metal surface at a given potential^{14,16} for electrochemical interfaces. Moreover, knowing the value of PZC can be useful to understand the pH effect on electrocatalysis. The difference between the applied potential and PZC determines the strength of electric field at the interface,^{17–20} which affects significantly the dynamics of water reorganization and the kinetics of proton transfer, and hence has impact on the electrocatalytic activity. This understanding was recently used by Koper and co-workers² for explaining the activity difference of HER in alkaline and acidic solution at Pt(111)/water interfaces, and it is supported by the experimental observation that lowering the PZC of Pt(111) by surface modification with Ni(OH)₂ effectively increases the HER activity in alkaline solution.

In view of the importance of PZC, many methods have been developed for determining PZC of metal/water interfaces. Experimentally, PZC can be obtained by measuring the maximum of surface tension,²¹ the Gouy–Chapman minimum,^{22–24} the potential of maximum entropy,²⁵ the amount of

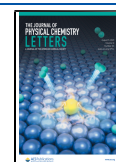
excess charge on surface (e.g., CO-displacement method),^{14,16} and so on. Alternatively, PZC can be determined with theoretical computation, and the advantage is that the clean metal/water interfaces can be readily modeled in the absence of contamination, while preparing a ultraclean single crystal surface is a major difficulty for PZC measurement in experiment. In the past few years, several groups^{26–31} have reported that the experimental values of the PZC of a variety of transition metal/water interfaces can be reproduced by simulating all-atom interface models using ab initio molecular dynamics (AIMD).

The PZC (U_{PZC}) of a metal/water interface is closely related to the work function of a metal surface (Φ_M),³² and as denoted in Figure 1(a), U_{PZC} and Φ_M differ by a Volta potential difference between the surface of metal and water ($\Delta\Phi$). $\Delta\Phi$ can also be interpreted as the change in Φ_M by adding liquid water onto a metal surface and can be measured by experiment.³⁴ It has been reported that $\Delta\Phi$ is dependent on the nature of the metal,³³ and the value of $\Delta\Phi$ is only -0.3 eV for most *sp* metals, while for transition metals like Pt and Pd, $\Delta\Phi$ can be as large as -1 eV. Recently, Le, Cheng et al.²⁶ have shown that the $\Delta\Phi$ for close-packed transition metal surfaces are mainly attributable to the induced dipole (*p*) due to electronic redistribution by water chemisorption, with little

Received: June 22, 2021

Accepted: July 26, 2021

Published: July 28, 2021



ACS Publications

© 2021 American Chemical Society

7299

<https://doi.org/10.1021/acs.jpclett.1c02001>
J. Phys. Chem. Lett. 2021, 12, 7299–7304

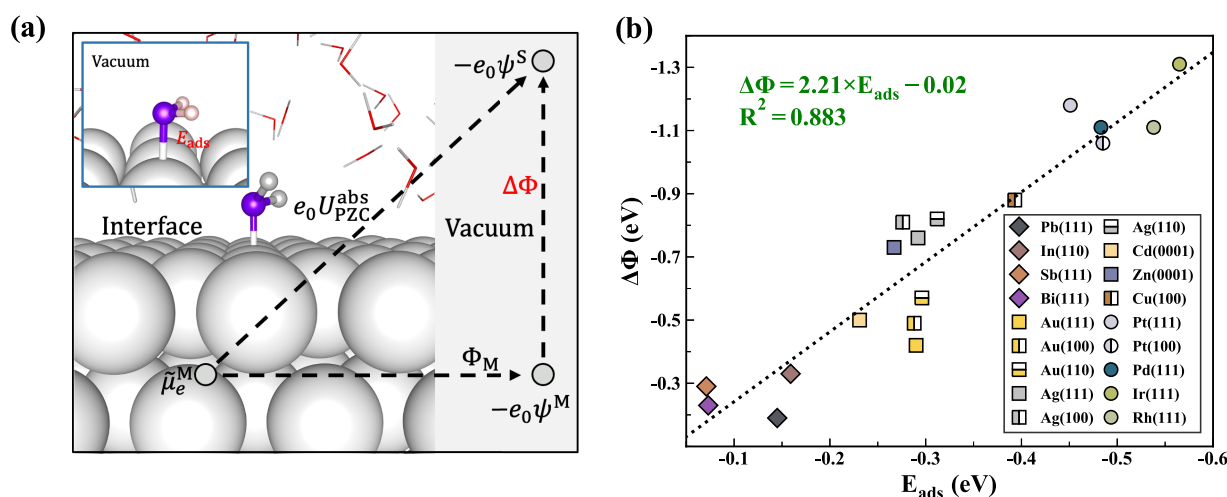


Figure 1. (a) The configurations of chemisorbed water on the metal surface in a vacuum and at the interface. Metal (i.e., Pt), H, O of chemisorbed water, and O of other water are colored in silver, white, purple, and red, respectively. The chemisorbed water is highlighted with the ball-and-stick model in comparison to other water with the line model. E_{ads} denotes for the adsorption energy of water on metal surface, and $U_{\text{PZC}}^{\text{abs}}$, Φ_M , and $\Delta\Phi$ represent the PZC at the absolute scale, the work function, and the Volta potential difference between the surface of metal and water, respectively. (b) The data points of $\Delta\Phi$ as a function of E_{ads} for 18 metal surfaces, fitted with a dotted line. The *sp*, *sd*, and *d* metals are marked in diamonds, squares, and circles, respectively. $\Delta\Phi$ are obtained from experimental data,^{34–43} and E_{ads} are calculated in this work.

contribution from orientational dipole at the PZC. Since chemisorbed water has a similar configuration (i.e., at top sites, see Figure 1(a)) on metal surfaces, one would expect that there may exist a correlation between $\Delta\Phi$ and E_{ads} with the latter relating to the chemisorption induced dipole.

By compiling $\Delta\Phi$ from experimental data^{34–43} and E_{ads} computed in this work for 18 low Miller index metal surfaces (see Table S1 and S2 in the Supporting Information), we interestingly find $\Delta\Phi$ has a good linear correlation with E_{ads} as shown in Figure 1(b). Note that the selected 18 metal surfaces include typical *sp*, *sd*, and *d* metals, and thus this relationship is likely to be universal for low Miller index metal surfaces. The fitted analytical expression shown in Figure 1(b) indicates at the weak adsorption limit (i.e., $E_{\text{ads}} = 0$), $\Delta\Phi$ would be close to 0, which is consistent with the previous finding that $\Delta\Phi$ is dominated by the electronic effect of water chemisorption.²⁶ It should be highlighted that this correlation offers an efficient way for quantifying $\Delta\Phi$, which only requires simple calculations of the adsorption energies in a vacuum, and thereby help estimate the PZC for other metal surfaces.

To understand the linear correlation between $\Delta\Phi$ and E_{ads} at the atomic level, we perform extensive AIMD simulations for 11 neutral metal/water interfaces at PZC conditions, including Pt(111), Pt(100), Pd(111), Cu(111), Cu(100), Zn(0001), Ag(111), Au(111), Pb(111), Cu(110), and Ag(110). Representative interface models are shown in Figure 2(a) and 2(b). As listed in Table 1, the corresponding electrode potentials are calculated with the computational standard hydrogen electrode (cSHE) method,^{26,33,44,45} which is briefly explained in the Supporting Information. It is encouraging to see that most computed PZC are in good agreement with experimental values. While for a few metal surfaces, e.g., Pt(100) and Pd(111), the computed PZC can deviate by ~ 0.5 V from experimental values. These errors are inherited from the underestimation of the work function Φ_M with PBE-D3 functional, and using $\Delta\Phi$ instead as the criteria for judging the accuracy of the simulated interfaces indicates that the standard PBE functional can well reproduce the experimental values of $\Delta\Phi$. We think this is because the

standard density functional is sufficiently accurate in describing the chemical interaction between water and the metal surface, thus leading to accurate electron redistribution and induced dipole, even though the work functions of some metal surfaces are underestimated.

The Volta potential difference $\Delta\Phi$ is often decomposed into two parts for the sake of theoretical understanding, i.e., the potential change caused by electron redistribution upon water chemisorption ($\Delta\Phi_{\text{el}}$) and the potential change due to water orientational dipole ($\Delta\Phi_{\text{ori}}$).^{26,32} We estimate $\Delta\Phi_{\text{el}}$ from electron redistribution profiles, and $\Delta\Phi_{\text{ori}}$ is computed by subtracting $\Delta\Phi_{\text{el}}$ from $\Delta\Phi$. Table 1 shows that $\Delta\Phi_{\text{ori}}$ has a very small contribution (within 0.2 eV) to $\Delta\Phi$ for all the studied metal surfaces, which is supported by the dipole orientation analysis shown in Figure 2(d) that the net orientational dipole of interface water integrated along the surface normal is close to zero. It should be noted that the orientational dipoles of ordered water layer models (e.g., the ice-like water bilayer), which are often used as simplified models for representing interface water,⁴⁶ can result in $\Delta\Phi_{\text{ori}}$ of more than ± 1 eV. This is significantly different from our AIMD simulations, indicating that these simplified models of interface water may be inappropriate for describing electrochemical interfaces at the PZC. In contrast to $\Delta\Phi_{\text{ori}}$, the term $\Delta\Phi_{\text{el}}$ makes dominating contribution to $\Delta\Phi$ for all computed metal surfaces. Table 1 shows the magnitude of $\Delta\Phi_{\text{el}}$ is strongly dependent on the nature of the metal surface, ranging from -0.2 eV to -1.3 eV (see Figure S6 for the convergence analysis of $\Delta\Phi_{\text{el}}$), as also manifested by the amount of partial electron transfer between water and metal surface shown in Figure 2(e).

Considering the relationship between $\Delta\Phi_{\text{el}}$ and chemisorbed water,²⁶ the density distribution profiles ($\rho_{\text{H}_2\text{O}}$) of chemisorbed water at different metal surfaces are analyzed, as shown in Figure 2(c). It is found that there is a distinct peak on Pt(111), Pt(100), Pd(111), Cu(111), Cu(100), and Cu(110) surfaces at $z < 2.75$ Å, which corresponds to the layer of chemisorbed water at the interfaces, and this assignment is supported by the orientation and density of

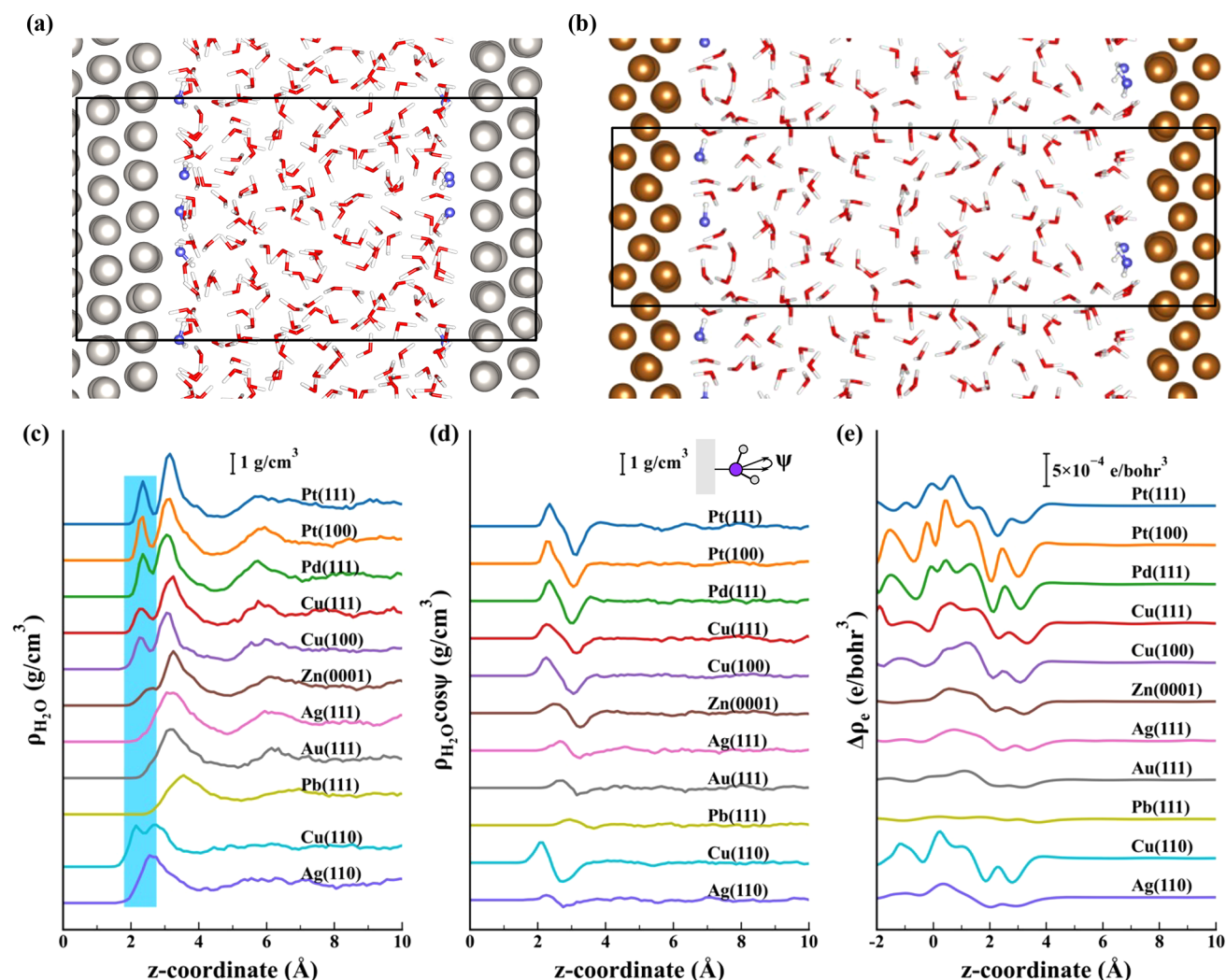


Figure 2. (a), (b) Models of the Pt(111)/water and Cu(110)/water interfaces. Pt, Cu, O, and H are colored in gray, brown, red, and white, respectively. The O atoms of chemisorbed water are highlighted in purple. (c)–(e) Distribution profiles of water density ($\rho_{\text{H}_2\text{O}}$), dipole orientation ($\rho_{\text{H}_2\text{O}} \cos \psi$), and electron density difference ($\Delta \rho_e$) along the surface normal (z-coordinate) at different metal/water interfaces. $\Delta \rho_e$ is calculated as $\Delta \rho_e = \rho_e(i) - \rho_e(M) - \rho_e(w)$, where $\rho_e(i)$, $\rho_e(M)$, and $\rho_e(w)$ denote the electron densities of the metal/water interface and metal and water separately, respectively. The zero in the z-coordinate corresponds to the uppermost layers of metal surfaces. The regions of chemisorbed water are indicated by a blue block in (c).

Table 1. Computed PZC vs SHE ($U_{\text{PZC}}^{\text{SHE}}$) and Work Functions (Φ_M) of 11 Metal Surfaces^a

surface	$U_{\text{PZC}}^{\text{SHE}}$	Φ_M/eV	$\Delta\Phi/\text{eV}$	$\Delta\Phi_{\text{el}}/\text{eV}$	$\Delta\Phi_{\text{ori}}/\text{eV}$
Pt(111)	0.2(0.3)	5.8(5.9)	−1.2(−1.2)	−1.3	0.1
Pt(100)	−0.1(0.3)	5.5(5.8)	−1.1(−1.1)	−1.2	0.1
Pd(111)	−0.5(0.1)	5.1(5.6)	−1.2(−1.1)	−1	−0.2
Cu(111)	−0.3(−0.7 ~ −0.2)	5.3(4.9)	−1.1(−1.2 ~ −0.7)	−1.0	−0.1
Cu(100)	−0.8(−0.7)	4.5(4.6)	−0.9(−0.9)	−0.8	−0.1
Zn(0001)	−0.9(−0.9)	4.4	−0.9	−0.7	−0.2
Ag(111)	−0.6(−0.5)	4.7(4.8)	−0.8(−0.7)	−0.7	−0.1
Au(111)	0.5(0.5)	5.4(5.4)	−0.5(−0.5)	−0.5	0
Pb(111)	−0.9(−0.6)	3.9	−0.4	−0.2	−0.2
Cu(110)	−0.9(−0.8)	4.6(4.5–4.9)	−1.1(−0.9 ~ −1.3)	−1.2	0.1
Ag(110)	−1.1(−0.7)	4(4.5)	−0.6(−0.8)	−0.8	0.2

^a $\Delta\Phi$ is the Volta potential difference between the surface of metal and water, and it can be decomposed into the change of interfacial potential from water orientation $\Delta\Phi_{\text{ori}}$ and electron redistribution $\Delta\Phi_{\text{el}}$. The data in the parentheses are recommended experimental values.^{34–43}

states (DOS) analysis of these water molecules in Figures S7 and S8. In contrast, this peak is not obvious on Zn(0001), Ag(111), Ag(110), Au(111), and Pb(111) surfaces since the

water adsorption energies on these surfaces are very low (> -0.32 eV) and surface water tends to form hydrogen bonds with other water molecules. Nevertheless, there is still a small

fraction of surface water chemisorbed on these metal surfaces, giving rise to the tails at $z < 2.75$ Å in the water density profiles on these metal surfaces. It should be mentioned that for two open surfaces, i.e., Cu(110) and Ag(110), a large fraction of water molecules distributed in the $z < 2.75$ Å region are not chemisorbed, which orient with one O–H bond pointing toward the metal surface and can be seen in the representative configuration shown in Figure 2(b). These water molecules have been excluded in counting for the coverage of chemisorbed water on metal surfaces.

Figure 3 plots the correlations of the computed $\Delta\Phi$, $\Delta\Phi_{\text{el}}$, and surface coverage of chemisorbed water (θ_A , the

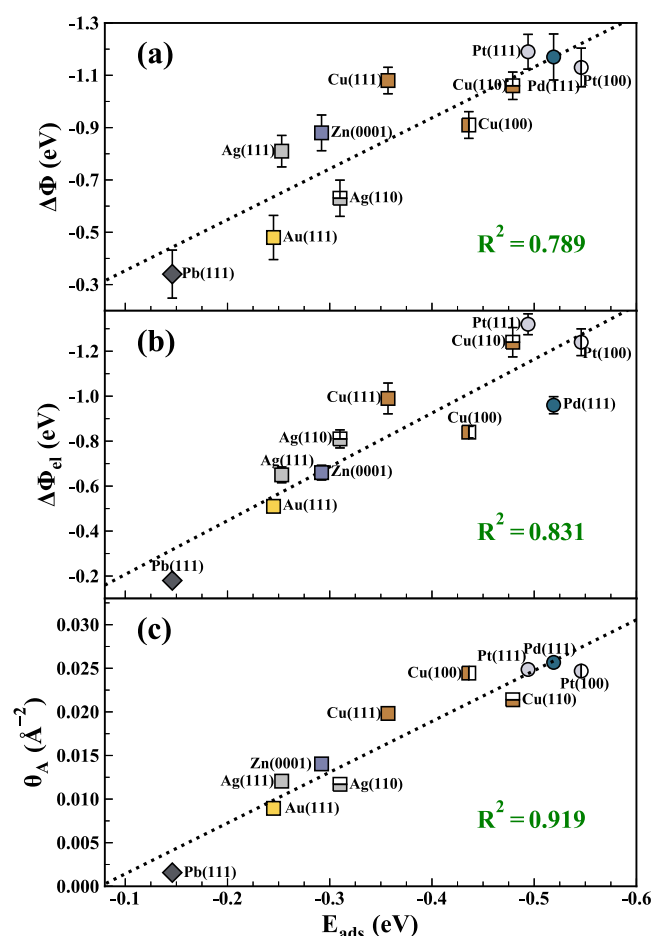


Figure 3. Correlations of the Volta potential difference between the surface of the metal and water $\Delta\Phi$ (a), interfacial potential change from electron redistribution $\Delta\Phi_{\text{el}}$ (b), and the coverage of chemisorbed water θ_A (c) computed by AIMD with water adsorption energy (E_{ads}) at 11 neutral metal/water interfaces. The dotted lines indicate the corresponding linear fits.

convergence of θ_A can be found in Figure S9) with E_{ads} . Note that θ_A in this work is defined as the number of chemisorbed water per unit area, rather than that per adsorption site often used,¹⁹ because the former is of more relevance to the present study. It can be seen from Figure 3(a) that since our computed $\Delta\Phi$ values are very close to experimental results, computed $\Delta\Phi$ has a similar linear correlation with E_{ads} (see also Figure 1(b)). Furthermore, $\Delta\Phi_{\text{el}}$ is also proportional to E_{ads} , as shown in Figure 3(b), because $\Delta\Phi_{\text{ori}}$ has negligible contribution to the interface potential.

It is also interesting to note from Figure 3(c) that the coverage of chemisorbed water θ_A linearly correlates with the adsorption energy E_{ads} , as one would expect from an adsorption isotherm at the intermediate coverage region.^{19,47} On the other hand, the magnitude of the induced dipole p is less sensitive to the nature of the metal surface. As shown in Figure S10, the values of the computed p are very close (i.e., -0.1 to -0.15 eÅ) on metal surfaces in a vacuum. Since $\Delta\Phi_{\text{el}}$ is proportional to $p \cdot \theta_A$, it is clear that the linear dependency of θ_A on E_{ads} is the main reason for the linear correlation between $\Delta\Phi_{\text{el}}$ and E_{ads} .

Thus, our work clearly shows there is a good linear relationship between $\Delta\Phi$ and E_{ads} , and moreover, this correlation should stem from the fact that the electronic component $\Delta\Phi_{\text{el}}$ linearly correlates with E_{ads} while the orientational component $\Delta\Phi_{\text{ori}}$ has a negligible contribution to $\Delta\Phi$. We demonstrate that this correlation is rather universal for metal–water interfaces and may be even transferable to other solid/liquid interfaces for understanding their corresponding PZC and band alignment.

In summary, we collect the experimental values of PZC and work functions of 18 metal surfaces and find that there is a linear correlation between the Volta potential difference $\Delta\Phi$ and water adsorption energy E_{ads} . We then simulate 11 metal/water interfaces at the PZC conditions using AIMD and compute their PZC with respect to SHE at good accuracy, thus confirming the linear correlation between $\Delta\Phi$ and E_{ads} . Detailed analyses indicate that this relation can be attributable to the fact that stronger adsorption of water leads to higher coverage of chemisorbed water at the PZC, and thus greater electronic dipole potential $\Delta\Phi_{\text{el}}$, while the orientational dipole of interface water is insignificant for all computed metal surfaces at the PZC. Finally, the observed linear correlation between E_{ads} and $\Delta\Phi$ can offer an efficient way to estimate the PZC of other metal surfaces. With proper further treatment, it may be even possible to extend this relation to metal alloys, which may be useful to help design alloy electrocatalysts with favorable PZC.

■ ASSOCIATED CONTENT

Supporting Information

The Supporting Information is available free of charge at <https://pubs.acs.org/doi/10.1021/acs.jpcclett.1c02001>.

Models of metal/water interfaces, computational setup for AIMD simulations, brief description of the cSHE method; figures of water configurations and metal/water interfaces, convergence analysis of Fermi level, electrostatic potential of bulk water, interface potential change caused by electron redistribution and coverage of chemisorbed water, density of states and angle distribution profiles of chemisorbed water, chemisorption induced dipole of each water on different metal surfaces, time evolution of total energy; tables of water adsorption energies, PZC, work functions, and Volta potential differences, and water densities (PDF)

■ AUTHOR INFORMATION

Corresponding Authors

Jia-Bo Le – Ningbo Institute of Materials Technology and Engineering, Chinese Academy of Sciences, Ningbo 315201, China; orcid.org/0000-0002-6570-5912; Email: lejiabo@nimte.ac.cn

Jun Cheng – State Key Laboratory of Physical Chemistry of Solid Surfaces, iChEM, College of Chemistry and Chemical Engineering, Xiamen University, Xiamen 361005, China;
orcid.org/0000-0001-6971-0797; Email: chengjun@xmu.edu.cn

Authors

Xiang-Ying Li – State Key Laboratory of Physical Chemistry of Solid Surfaces, iChEM, College of Chemistry and Chemical Engineering, Xiamen University, Xiamen 361005, China

Ao Chen – State Key Laboratory of Physical Chemistry of Solid Surfaces, iChEM, College of Chemistry and Chemical Engineering, Xiamen University, Xiamen 361005, China

Xiao-Hui Yang – State Key Laboratory of Physical Chemistry of Solid Surfaces, iChEM, College of Chemistry and Chemical Engineering, Xiamen University, Xiamen 361005, China

Jia-Xin Zhu – State Key Laboratory of Physical Chemistry of Solid Surfaces, iChEM, College of Chemistry and Chemical Engineering, Xiamen University, Xiamen 361005, China;
orcid.org/0000-0002-3471-4728

Complete contact information is available at:

<https://pubs.acs.org/10.1021/acs.jpcllett.1c02001>

Notes

The authors declare no competing financial interest.

ACKNOWLEDGMENTS

We are grateful for the financial support from the National Natural Science Foundation of China (Grant Nos. 21991151, 21991150, 21861132015, 22021001, and 21902136) and the Principal's fund of Xiamen University (Grant No. 20720190047).

REFERENCES

- (1) Subbaraman, R.; Tripkovic, D.; Strmcnik, D.; Chang, K.-C.; Uchimura, M.; Paulikas, A. P.; Stamenkovic, V.; Markovic, N. M. Enhancing Hydrogen Evolution Activity in Water Splitting by Tailoring Li⁺-Ni(OH)₂-Pt Interfaces. *Science* **2011**, *334*, 1256–1260.
- (2) Ledezma-Yanez, I.; Wallace, W. D. Z.; Sebastián-Pascual, P.; Climent, V.; Feliu, J. M.; Koper, M. T. M. Interfacial water reorganization as a pH-dependent descriptor of the hydrogen evolution rate on platinum electrodes. *Nat. Energy* **2017**, *2*, 17031.
- (3) Dubouis, N.; Grimaud, A. The hydrogen evolution reaction: from material to interfacial descriptors. *Chem. Sci.* **2019**, *10*, 9165–9181.
- (4) Zheng, J.; Sheng, W.; Zhuang, Z.; Xu, B.; Yan, Y. Universal dependence of hydrogen oxidation and evolution reaction activity of platinum-group metals on pH and hydrogen binding energy. *Sci. Adv.* **2016**, *2*, No. e1501602.
- (5) Kulkarni, A.; Siahrostami, S.; Patel, A.; Nørskov, J. K. Understanding Catalytic Activity Trends in the Oxygen Reduction Reaction. *Chem. Rev.* **2018**, *118*, 2302.
- (6) Nayak, S.; McPherson, I. J.; Vincent, K. A. Adsorbed Intermediates in Oxygen Reduction on Platinum Nanoparticles Observed by In Situ IR Spectroscopy. *Angew. Chem., Int. Ed.* **2018**, *57*, 12855–12858.
- (7) Li, J.; Yin, H.-M.; Li, X.-B.; Okunishi, E.; Shen, Y.-L.; He, J.; Tang, Z.-K.; Wang, W.-X.; Yücelen, E.; Li, C.; et al. Surface evolution of a Pt–Pd–Au electrocatalyst for stable oxygen reduction. *Nat. Energy* **2017**, *2*, 17111.
- (8) Wang, Y.-H.; Le, J.-B.; Li, W.-Q.; Wei, J.; Radjenovic, P.; Zhang, H.; Zhou, X.-S.; Cheng, J.; Tian, Z.-Q.; Li, J.-F. In situ Spectroscopic Insight into the Origin of the Enhanced Performance of Bimetallic nanocatalysts towards ORR. *Angew. Chem., Int. Ed.* **2019**, *58*, 16062.

- (9) Nitopi, S.; Bertheussen, E.; Scott, S. B.; Liu, X.; Engstfeld, A. K.; Horch, S.; Seger, B.; Stephens, I. E. L.; Chan, K.; Hahn, C.; et al. Progress and Perspectives of Electrochemical CO₂ Reduction on Copper in Aqueous Electrolyte. *Chem. Rev.* **2019**, *119*, 7610–7672.
- (10) Cheng, T.; Xiao, H.; Goddard, W. A. Reaction Mechanisms for the Electrochemical Reduction of CO₂ to CO and Formate on the Cu(100) Surface at 298 K from Quantum Mechanics Free Energy Calculations with Explicit Water. *J. Am. Chem. Soc.* **2016**, *138*, 13802–13805.
- (11) Ma, W.; Xie, S.; Liu, T.; Fan, Q.; Ye, J.; Sun, F.; Jiang, Z.; Zhang, Q.; Cheng, J.; Wang, Y. Electrocatalytic reduction of CO₂ to ethylene and ethanol through hydrogen-assisted C–C coupling over fluorine-modified copper. *Nat. Catal.* **2020**, *3*, 478–487.
- (12) Li, F.; Thevenon, A.; Rosas-Hernández, A.; Wang, Z.; Li, Y.; Gabardo, C. M.; Ozden, A.; Dinh, C. T.; Li, J.; Wang, Y.; et al. Molecular tuning of CO₂-to-ethylene conversion. *Nature* **2020**, *577*, 509–513.
- (13) Petrii, O. A. Zero charge potentials of platinum metals and electron work functions (Review). *Russ. J. Electrochem.* **2013**, *49*, 401.
- (14) Cuesta, A. Measurement of the surface charge density of CO-saturated Pt(111) electrodes as a function of potential: The potential of zero charge of Pt(111). *Surf. Sci.* **2004**, *572*, 11.
- (15) Frumkin, A. N.; Petrii, O. A. Potentials of zero total and zero free charge of platinum group metals. *Electrochim. Acta* **1975**, *20*, 347.
- (16) Rizo, R.; Sitta, E.; Herrero, E.; Climent, V.; Feliu, J. M. Towards the understanding of the interfacial pH scale at Pt(111) electrodes. *Electrochim. Acta* **2015**, *162*, 138.
- (17) Le, J.-B.; Chen, A.; Li, L.; Xiong, J.-F.; Lan, J.; Liu, Y.-P.; Iannuzzi, M.; Cheng, J. Modeling Electrified Pt(111)-Had /Water Interfaces from Ab Initio Molecular Dynamics. *JACS Au* **2021**, *1*, 569–577.
- (18) Li, C.-Y.; Le, J.-B.; Wang, Y.-H.; Chen, S.; Yang, Z.-L.; Li, J.-F.; Cheng, J.; Tian, Z.-Q. In situ probing electrified interfacial water structures at atomically flat surfaces. *Nat. Mater.* **2019**, *18*, 697.
- (19) Le, J.-B.; Fan, Q.-Y.; Li, J.-Q.; Cheng, J. Molecular origin of negative component of Helmholtz capacitance at electrified Pt(111)/water interface. *Sci. Adv.* **2020**, *6*, No. eabb1219.
- (20) Le, J.; Cuesta, A.; Cheng, J. The structure of metal-water interface at the potential of zero charge from density functional theory-based molecular dynamics. *J. Electroanal. Chem.* **2018**, *819*, 87.
- (21) Fredlein, R. A.; Damjanovic, A.; Bockris, J. O. Differential surface tension measurements at thin solid metal electrodes. *Surf. Sci.* **1971**, *25*, 261–264.
- (22) Valette, G. Double layer on silver single crystal electrodes in contact with electrolytes having anions which are slightly specifically adsorbed. Part III. The (111) face. *J. Electroanal. Chem. Interfacial Electrochem.* **1989**, *269*, 191.
- (23) Kolb, D. M.; Schneider, J. Surface reconstruction in electrochemistry: Au(100)-(5*20), Au(111)-(1*23) and Au(110)-(1*2). *Electrochim. Acta* **1986**, *31*, 929.
- (24) Ojha, K.; Arulmozhi, N.; Aranzales, D.; Koper, M. T. M. Double Layer of Pt(111)-Aqueous Electrolyte Interface: Potential of Zero Charge and Anomalous Gouy-Chapman Screening. *Angew. Chem., Int. Ed.* **2020**, *59*, 711.
- (25) Sebastián, P.; Martínez-Hincapié, R.; Climent, V.; Feliu, J. M. Study of the Pt (111) electrolyte interface in the region close to neutral pH solutions by the laser induced temperature jump technique. *Electrochim. Acta* **2017**, *228*, 667–676.
- (26) Le, J.; Iannuzzi, M.; Cuesta, A.; Cheng, J. Determining potentials of zero charge of metal electrodes versus the standard hydrogen electrode from based on density-functional-theory-based molecular dynamics. *Phys. Rev. Lett.* **2017**, *119*, 16801.
- (27) Bouzid, A.; Pasquarello, A. Atomic-Scale Simulation of Electrochemical Processes at Electrode/Water Interfaces under Referenced Bias Potential. *J. Phys. Chem. Lett.* **2018**, *9*, 1880.
- (28) Sakong, S.; Forster-Tonigold, K.; Groß, A. The structure of water at a Pt(111) electrode and the potential of zero charge studied from first principles. *J. Chem. Phys.* **2016**, *144*, 194701.

- (29) Bramley, G.; Nguyen, M. T.; Glezakou, V. A.; Rousseau, R.; Skylaris, C. K. Reconciling Work Functions and Adsorption Enthalpies for Implicit Solvent Models: A Pt (111)/Water Interface Case Study. *J. Chem. Theory Comput.* **2020**, *16*, 2703–2715.
- (30) Li, P.; Huang, J.; Hu, Y.; Chen, S. Establishment of the Potential of Zero Charge of Metals in Aqueous Solutions: Different Faces of Water Revealed by Ab Initio Molecular Dynamics Simulations. *J. Phys. Chem. C* **2021**, *125*, 3972–3979.
- (31) Le, J.; Fan, Q.; Perez-Martinez, L.; Cuesta, A.; Cheng, J. Theoretical insight into the vibrational spectra of metal-water interfaces from density functional theory based molecular dynamics. *Phys. Chem. Chem. Phys.* **2018**, *20*, 11554.
- (32) Schmickler, W.; Santos, E. *Interfacial Electrochemistry*, 2nd ed.; Springer Berlin Heidelberg: Berlin, Heidelberg, 2010; pp 1–267.
- (33) Le, J.-B.; Cheng, J. Modeling electrochemical interfaces from ab initio molecular dynamics: water adsorption on metal surfaces at potential of zero charge. *Curr. Opin. Electrochem.* **2020**, *19*, 129–136.
- (34) Trasatti, S.; Lust, E. *Modern Aspects of Electrochemistry* No. 33; Kluwer Academic Publishers, 2002; pp 1–215.
- (35) Derry, G. N.; Kern, M. E.; Worth, E. H. Recommended values of clean metal surface work functions. *J. Vac. Sci. Technol., A* **2015**, *33*, 060801.
- (36) El-Aziz, A. M.; Kibler, L. A.; Kolb, D. M. The potentials of zero charge of Pd(111) and thin Pd overlayers on Au(111). *Electrochem. Commun.* **2002**, *4*, 535.
- (37) Łukomska, A.; Sobkowski, J. Potential of zero charge of monocrystalline copper electrodes in perchlorate solutions. *J. Electroanal. Chem.* **2004**, *567*, 95–102.
- (38) Auer, A.; Ding, X.; Bandarenka, A. S.; Kunze-Liebhäuser, J. The Potential of Zero Charge and the Electrochemical Interface Structure of Cu(111) in Alkaline Solutions. *J. Phys. Chem. C* **2021**, *125*, 5020–5028.
- (39) Himpsel, F. J.; Eastman, D. E.; Koch, E. E. Free-electron-like bulk and surface states for Zn(0001). *Phys. Rev. B: Condens. Matter Mater. Phys.* **1981**, *24*, 1687–1690.
- (40) Michaelson, H. B. The work function of the elements and its periodicity. *J. Appl. Phys.* **1977**, *48*, 4729.
- (41) Lang, N. D.; Kohn, W. Theory of metal surfaces: Work function. *Phys. Rev. B* **1971**, *3*, 1215–1223.
- (42) Kawano, H. Effective work functions for ionic and electronic emissions from mono- and polycrystalline surfaces. *Prog. Surf. Sci.* **2008**, *83*, 1–165.
- (43) Muntwiler, M.; Zhu, X. Y. Image-potential states on the metallic (111) surface of bismuth. *New J. Phys.* **2008**, *10*, 113018.
- (44) Cheng, J.; Liu, X.; VandeVondele, J.; Sulpizi, M.; Sprik, M. Redox potentials and acidity constants from density functional theory based molecular dynamics. *Acc. Chem. Res.* **2014**, *47*, 3522.
- (45) Cheng, J.; Sprik, M. Alignment of electronic energy levels at electrochemical interfaces. *Phys. Chem. Chem. Phys.* **2012**, *14*, 11245.
- (46) Schnur, S.; Groß, A. Properties of metal-water interfaces studied from first principles. *New J. Phys.* **2009**, *11*, 125003.
- (47) Gileadi, E. *Physical Electrochemistry. Fundamentals, Techniques and Applications*; Wiley-VCH, 2011; pp 1–374.